Optik 127 (2016) 1022–1026

Contents lists available at ScienceDirect

Optik

journal homepage: www.elsevier.de/ijleo

Design of an all-reflective active zoom system

Xi Wang [a], Jun Chang [a,*], Benlan Shen [a], Weiyi Zha [a], Yajun Niu [a], Ke Zhang [b], Shulong Feng [c]

[a] Beijing Institute of Technology, School of Opto-electronics, South Zhongguancun Street Haidian District, Beijing 100081, China
[b] China North Vehicle Research Institute, No. 4 Huaishuling, Fengtai District, Beijing 100072, China
[c] Changchun Institute of Optics, Fine Mechanics and Physics, Chinese Academy of Sciences, Dong Nanhu Road 3888, Changchun 130033, Jilin, China

ARTICLE INFO

Article history:
Received 22 November 2014
Accepted 26 September 2015

Keywords:
Reflective zooms
Three mirrors
Deformable mirror
Seidel aberration theory
Optical design

ABSTRACT

Based on active optics, the zoom system design can no longer be confined to traditional methods of changing the distances between optical components for variable focal lengths. An all-reflective active zoom system with three mirrors is designed. The primary and third aspheric mirrors act as deformable mirrors to realize the transition among the different focal lengths by the curvature radius variation, while the second aspheric mirror is static. According to the third-order aberration theory and dimension calculations of the optical system requirements with the constraint limitations, the system's initial construction parameters can be achieved. This all-reflective active zoom system can realize zoom ratio is 3, focal length between 5 and 15 mm, field-of-view of 10–27.8°, and wide working wavelength from the visible to infrared.

1. Introduction

In the past few years, zooming system research has attracted much attention. Currently, there are two zooming methods: the optical and the digital. The optical zoom essentially varies the system effective focal length by adjusting the separation between individual and group components. Conversely, the digital zoom only increases the pixel size of the image without varying the image optical information. The varifocal systems in these two zooming methods are distinct from each other, and each one has its own advantages and disadvantages. Recently, zooming system research focus moved from the traditional zoom lens to the reflective mechanical and active zooming modes. The traditional zoom system, which consists of refractive lenses, usually varies the focal length or magnification with the spaces between lenses, while the reflective mechanical zoom system with mirrors uses the same zoom method but avoids chromatic aberrations. In addition, the active zoom system has control flexibility because it can achieve focal length variation without moving any elements [1,2]. An all-reflective active zoom system, which combines the above advantages, can finally eliminate chromatic aberrations and component movement [3].

To reduce or eliminate the image plane shift, optical zoom systems adopt two compensation methods: mechanical and optical. The mechanical compensation allows each component to move individually under different rules, while optical compensation requires that all the movable components move under identical rules. Optical zooming is easier to realize and more useful than mechanical zooming because it uses an accurate camera to ensure the accuracy of the movable groups' motion. Previously, mechanical compensation was common in zoom systems, but it was time consuming. Recently, the reflective active zoom system has attracted much attention [4,5]. The active zoom concept creates changes in the effective focal length by only leveraging the individual element's focal length, which is much more convenient and simpler than the typical mechanical compensation zooming method. These zoom systems are capable of being varifocal without moving components by incorporating active optical elements such as deformable mirrors or liquid lenses [6]. These active elements do not waste time on mechanical motion because they use a voltage to vary their focal lengths [7,8]. However, the variable range of these element focal lengths is so limited that it is difficult to achieve high zoom ratios.

This paper proposes the design of the following two systems: an all-reflective coaxial zoom and an off-axis system. In addition, the imaging properties of the reflective system are discussed based on the third-order aberration theory. The image quality results indicate that the new systems meet the design requirements. As such, the proposed designs of the two systems can serve as a reference for other similar systems.

2. Three-mirror system first-order design theory

The collinear optical system model with three elements is shown in Fig. 1. Each element is assumed to have zero thickness.

* Corresponding author. Tel.: +86 13611044240.
E-mail address: bitchang@bit.edu.cn (J. Chang).

http://dx.doi.org/10.1016/j.ijleo.2015.09.188
0030-4026/

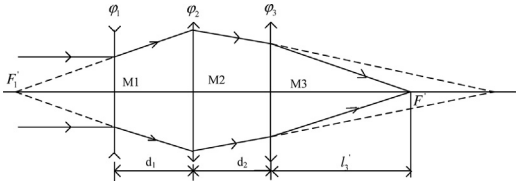

Fig. 1. Schematic diagram of a collinear optical system structure.

Based on the Matrix Optics theory, the paraxial ray tracing will be used as follows. Consider a system of three alternately stationary and deformable elements arranged along a common optical axis, as shown in Fig. 1. Here, M_1, M_2, M_3 represent the three mirrors; F_1' is the first focus of M_1; F_1' is the second focus of the system; φ_1, φ_2, and φ_3 represent three components' optical powers; d_1 and d_2 represent the distances between M_1M_2 and M_2M_3; and l_3' is the back focal length of the system. In the following analysis, the designations of the optical components are chosen in ascending order from the object side to the image side. Each component, having either a negative or positive power, is represented in Fig. 1 by a hypothetical thin lens. The first element, which varies its curvature when the system is zooming, has a negative power, i.e., it diverges the narrow field incident rays, while the second and third mirrors have positive powers, i.e., they converge the divergent rays. The radius of the third element is also variable to compensate for the image surface shift during system zooming. Obviously, the primary and third mirrors are responsible for realizing zooming by changing curvatures, rather than the spaces between the components. Thus, the system's back focal length will be identical for different optical powers.

The system in Fig. 1 is an inverted-telephoto-type system, consisting of a negative primary mirror M_1 and rear positive mirror group, M_2M_3. The inverted telephoto type is intended to realize a large field of view. M_1, which has a positive power, is used to converge the divergent beam. Meanwhile, the focal lengths of the primary and third elements are used for zooming and compensating for the image plane shift, respectively. As such, optical zooming is much different from the mechanical zooming and more convenient to control.

The paraxial imaging theory of a collinear system with three optical components can be described by a 2×2 matrix calculation process. Each component will be expressed as:

$$\phi_1 = \begin{pmatrix} 1 & 0 \\ -\phi_1 & 1 \end{pmatrix}, \quad \phi_2 = \begin{pmatrix} 1 & 0 \\ -\phi_2 & 1 \end{pmatrix}, \quad \phi_3 = \begin{pmatrix} 1 & 0 \\ -\phi_3 & 1 \end{pmatrix}, \quad (1)$$

where ϕ_1, ϕ_2, and ϕ_3 are three matrices. Then the optical powers of mirrors φ_i can be written as

$$\varphi_1 = \frac{1}{f_1'}, \quad \varphi_2 = \frac{1}{f_2'}, \quad \varphi_3 = \frac{1}{f_3'}, \quad (2)$$

where f_1', f_2', and f_3' represent the focal lengths of the mirrors. The spaces between every two elements can be written as:

$$T_1 = \begin{pmatrix} 1 & d_1 \\ 0 & 1 \end{pmatrix}, \quad T_2 = \begin{pmatrix} 1 & d_2 \\ 0 & 1 \end{pmatrix} \quad (3)$$

where T_1 and T_2 are two matrices. The matrix for the overall paraxial system M can be calculated using

$$M = \begin{pmatrix} A & B \\ C & D \end{pmatrix} = \phi_3 T_2 \phi_2 T_1 \phi_1 = \begin{pmatrix} 1 & 0 \\ -\varphi_3 & 1 \end{pmatrix} \begin{pmatrix} 1 & d_2 \\ 0 & 1 \end{pmatrix} \begin{pmatrix} 1 & 0 \\ -\varphi_2 & 1 \end{pmatrix} \begin{pmatrix} 1 & d_1 \\ 0 & 1 \end{pmatrix} \begin{pmatrix} 1 & 0 \\ -\varphi_1 & 1 \end{pmatrix} \quad (4)$$

where

$$A = 1 - d_2 * \varphi_2 - ((1 - d_2 * \varphi_2) * d_1 + d_2) * \varphi_1 \quad (5)$$

$$B = (1 - d_2 * \varphi_2) * d_1 + d_2 \quad (6)$$

$$C = -\varphi_3 - (-\varphi_3 * d_2 + 1) * \varphi_2 - ((-\varphi_3 - (-\varphi_3 * d_2 + 1) * \varphi_2) * d_1 - \varphi_3 * d_2 + 1) * \varphi_1 \quad (7)$$

$$D = (-\varphi_3 - (-\varphi_3 * d_2 + 1) * \varphi_2) * d_1 - \varphi_3 * d_2 + 1 \quad (8)$$

The optical system power f' and back focal length l_3' of the collinear system with three optical components can be described by ABCD matrix as:

$$f' = -\frac{1}{C} = -\frac{1}{-\varphi_3 - (-\varphi_3 * d_2 + 1) * \varphi_2 - ((-\varphi_3 - (-\varphi_3 * d_2 + 1) * \varphi_2) * d_1 - \varphi_3 * d_2 + 1) * \varphi_1}, \quad (9)$$

$$l_3' = -\frac{A}{C} = f'A = f'(1 - d_2 * \varphi_2 - ((1 - d_2 * \varphi_2) * d_1 + d_2) * \varphi_1) \quad (10)$$

To keep the image plane stationary, l_3' will remain unchanged when the focal length of the active zoom system is changing, which means $l_3' = a$ (constant). In this three-component system, ray tracing will be confined by the above constraints. According to the practical requirements and Gaussian Optics theory, the system collects a set of Seidel aberration coefficient functions:

$$S_{ki} = S_{ki}\left(f_{1i}', f_2', f_{3i}', \beta_{2i}, \beta_{3i}\right) \quad (11)$$

where i is a multiplet of the active zoom system. $k = 1, 2, 3, 4$ and S_{1i}, S_{2i}, S_{3i}, and S_{4i} represent the system spherical aberration, coma, astigmatism and field curvature, respectively. β_{2i} and β_{3i} represent the magnifications between M_1M_2 and M_2M_3, respectively. When the active zoom system has different focal lengths due to the surface curvature changes of M_1 and M_3, f_{1i}', f_{3i}', β_{2i}, and β_{3i} will also change.

Accordingly, the first and third mirror powers can be expressed as: $\varphi_{1i} = 1/f_{1i}'$, $\varphi_{3i} = 1/f_{3i}'$. The active zoom system focal length can be written as:

$$F_i' = -\frac{1}{-\varphi_{3i} - (-\varphi_{3i} * d_2 + 1) * \varphi_2 - ((-\varphi_{3i} - (-\varphi_{3i} * d_2 + 1) * \varphi_2) * d_1 - \varphi_{3i} * d_2 + 1)) * \varphi_{1i}} \quad (12)$$

where $F_{(2-3)i}$ represents the focal power combination of the second and third mirrors, $F_{(2-3)i} > 0$.

3. Three-mirror active zoom system design

According to the theory mentioned above, the three-mirror active zoom system will be designed as follows. The system zoom ratio is 3; the focal length will be 5, 10, and 15 mm; and field of

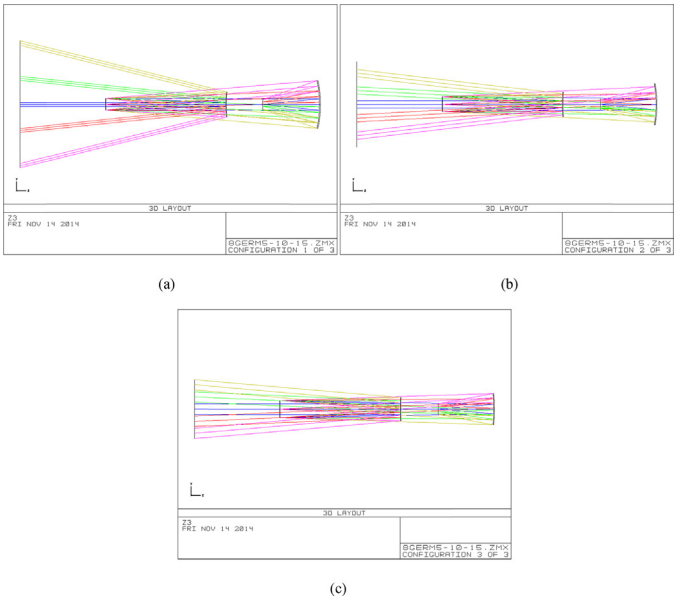

Fig. 2. The layout of the coaxial active zoom optical system for a focal length of (a) 5, (b) 10, and (c) 15 mm.

view will be 10–27.8°. Then, the system initial parameters will be decided as follows

$$\begin{cases} F_1' = 5\,\text{mm}, \\ F_2' = 10\,\text{mm}, \\ F_3' = 15\,\text{mm}, \\ f_{3i}'\left[f_2' * \left(f_{1i}' - d_1\right) - d_2 * \left(f_{1i}' - d_1 - f_2'\right)\right] \\ \quad = a * \left[f_2' * \left(f_{1i}' - d_1\right) - \left(d_3 + f_{3i}'\right) * \left(f_{1i}' - d_1 - f_2'\right)\right], \\ \quad (\text{“a” is a constant}) \\ S_{ki} = S_{ki}\left(f_{1i}', f_2', f_{3i}', \beta_{2i}, \beta_{3i}\right), \\ \varphi_{1i} < 0, \\ F_{(2-3)i} > 0. \end{cases} \tag{13}$$

From Eq. (13), the initial system structure will be obtained. Owing to the large field of view, it is difficult to correct the system aberrations. As a result, the aspheric coefficients must be introduced into the system. The primary, second, and third mirrors are all aspherical in the active zooming system. The primary and third mirrors have different curvature radius values when the system has different focal lengths. Currently available, deformable mirrors and other active optical elements lack the maximum center stroke and number of pixels necessary to adequately change the focal length of the individual elements. As such, these commercial deformable mirrors do not meet our requirements. Therefore, we use several independent mirrors that have fixed curvatures to simulate the deformable mirror for the system with focal lengths of 5, 10, and 15 mm.

The coaxial active zoom optical system layouts with different focal lengths are shown in Fig. 2. The specifications are listed in

Table 1
System parameters.

	Zoom 1	Zoom 2	Zoom 3
f (mm)	5	10	15
F (#)	4.99	5.07	6.04
Spectral range (μm)	0.486–1.064		
Field of view	−13.9–13.9°	−6.75–6.75°	−5–5°

Table 2
Radius of curvature.

Mirror	Zoom 1	Zoom 2	Zoom 3
1	33.4	49.3	98.6
2	75.8		
3	−31.7	−32.8	−34.5

Table 3
Displacement between mirrors.

Mirror 1–Mirror 2 (mm)	−20.7
Mirror 2–Mirror 3 (mm)	31.9
Mirror 3–Image (mm)	−16.1

Tables 1–3. Figs. 3 and 4 show the quality of the system imaging for focal lengths of 5, 10 and 15 mm. The system imaging quality analysis shows that spherical and coma aberrations are relatively large. Furthermore, the system obscuration ratio is too large to ensure a sufficient luminous flux. From the coaxial system layout, it is obvious that the most or all of the rays will be intercepted while propagating from the second to the third mirrors. Thus, the energy will be insufficient for imaging at the image plane. This indicates that the coaxial active zoom optical system structure will be of no practical significance and will require an off-axis reflective optical system.

To solve the obscuration problem, the field will be derived and mirrors will be tilted in the off-axis system. There will be no light blocked by the optical elements when the imaging rays propagate from the primary mirror to the image plane. However, the elements tilting can introduce off-axis aberrations, which will result in the degradation of system imaging quality. As such, higher order aspheric coefficients are required to correct the off-axis aberrations. Therefore, the off-axis active zooming system involves both the optical components tilting and high order aspheric coefficients machining. In addition, the assembly is quite difficult.

The off-axis active zoom optical system layouts with the different focal lengths are shown in Fig. 5. Similarly, Figs. 6 and 7 show the quality of system imaging for the three different focal lengths. Table 4 provides the system parameters. The imaging quality analysis shows that the spherical, coma, and astigmatism aberrations

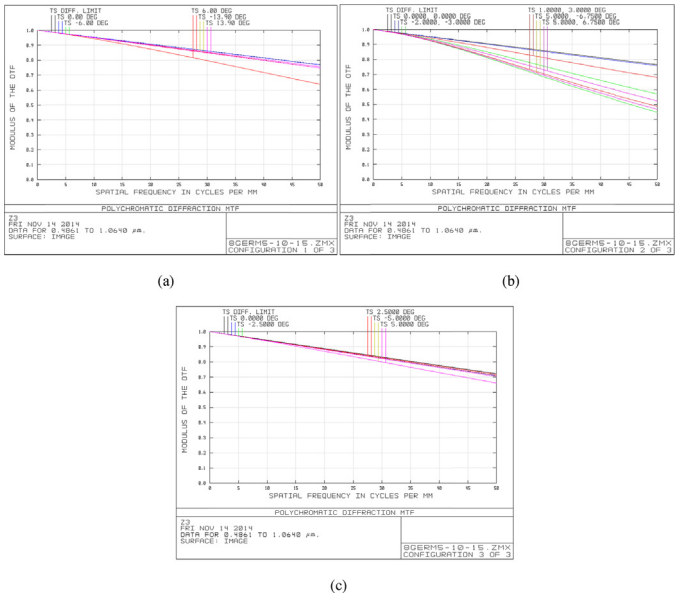

Fig. 3. The MTF of the coaxial active zoom optical system for a focal length of (a) 5, (b) 10, and (c) 15 mm.

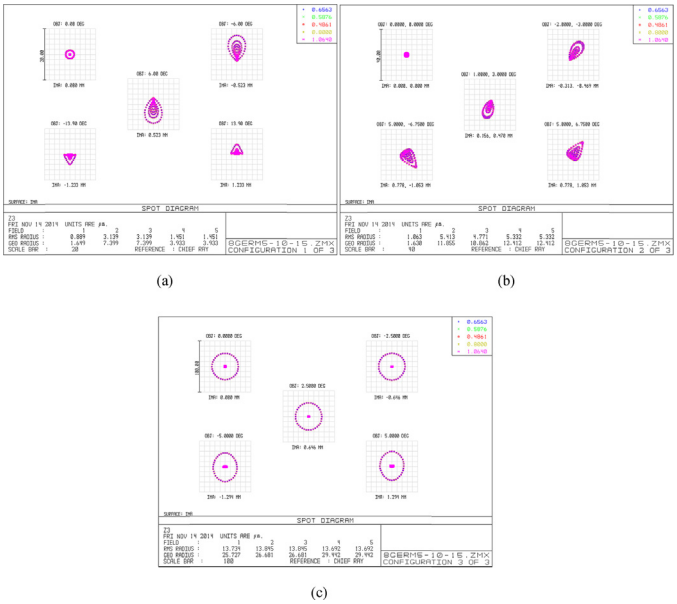

Fig. 4. The spot diagram of the coaxial active zoom optical system for a focal length of (a) 5, (b) 10, and (c) 15 mm.

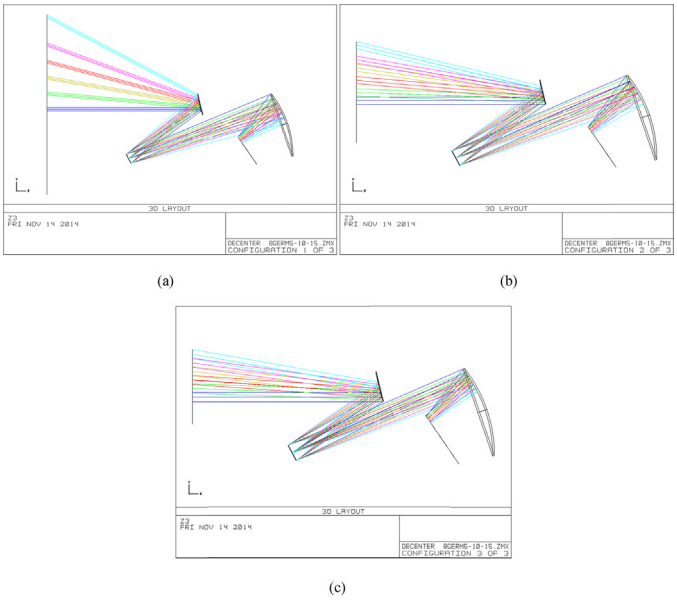

Fig. 5. The layout of the off-axis active zoom optical system for a focal length of (a) 5, (b) 10, and (c) 15 mm.

Table 4
System parameters.

		Zoom 1	Zoom 2	Zoom 3
f (mm)		5	10	15
F (#)		4.94	4.74	5.93
Spectral range (μm)		0.486–1.064		
Field of view		−27.8–0°	−13.5–0°	−10–0°
Image height (mm)	X	1.68	3.01	4.34
	Y	1.75	3.14	4.53

exist in the system. However, the off-axis active zooming system is without obscuration. Accordingly, the image receiver can get sufficient energy at the image plane.

Comparing the coaxial and off-axis active zoom optical systems, we found that the aberrations of the two structures are similar. However, the off-axis system image performances are overall

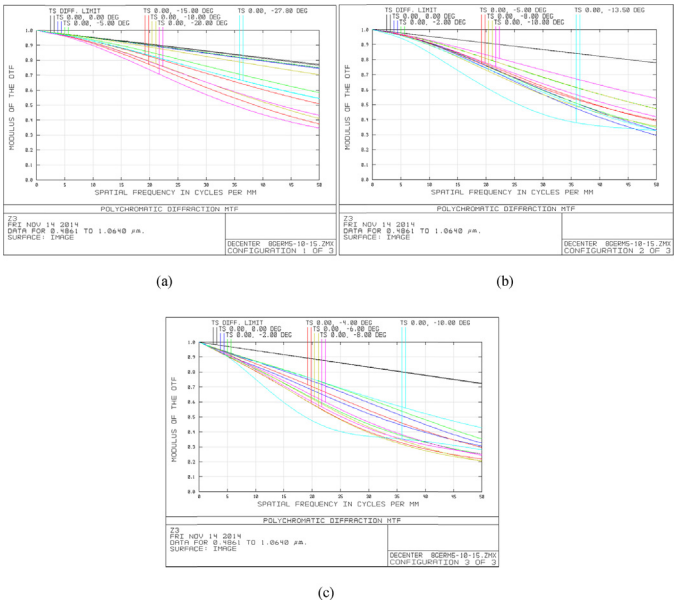

Fig. 6. The MTF of the off-axis active zoom optical system for a focal length of (a) 5, (b) 10, and (c) 15 mm.

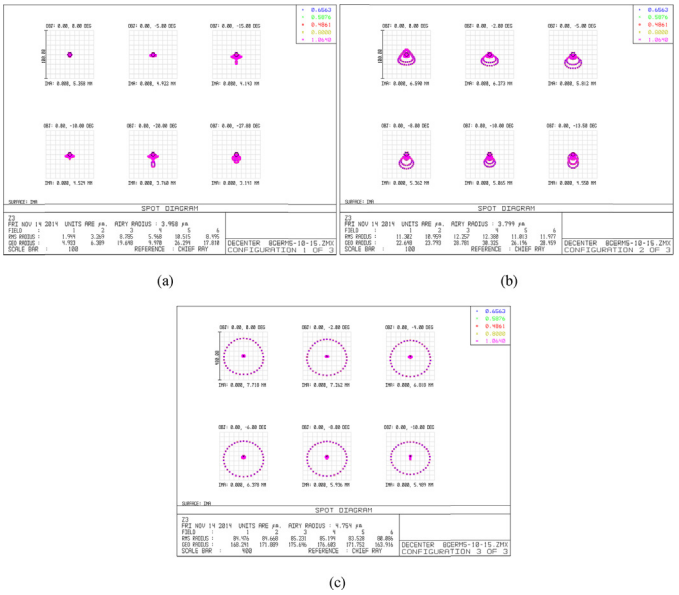

Fig. 7. The spot diagram of the off-axis active zoom optical system for a focal length of (a) 5, (b) 10, and (c) 15 mm.

worse than the coaxial one because off-axis aberrations exist in the off-axis system and need to be further improved.

4. Conclusions

The reflective active zoom system researched in this study mainly focuses on two points: keeping the image plane stable and balancing the system total image performance during zooming, which result from variations in elements' curvature. The system aberration balance is the basis for initial system structure and optimization. Moreover, high order aspheric coefficients are adaptive in this system. Aspheric surface precision and off-axis system assembly, however, are the two main technical difficulties associated with this system. To improve the applicability of the active zoom

system, further research on the system proposed in the present work is required.

Acknowledgments

This work is supported by a program for New Century Excellent Talents in University 2012cx01017 from the Ministry of Education. The work is also partially supported by the financial assistance of the Major Project Cultivation Fund, 2205020 of Beijing Institute of Technology. It is also supported by a program for National Natural Science Foundation of China 61178041. The project is also supported by Key Laboratory of Photoelectronic Imaging Technology and System, Beijing Institute of Technology, Ministry of Education of the People's Republic of China, 2014OEIOF03.

References

[1] M.E.L. Jungwirth, D.V. Wick, E.L. Dereniak, Theory and tradespace analysis of a reflective axial adaptive optical zoom system, Opt. Eng. 51 (8) (2012) 083001.
[2] W.B. Wetherell, M.P. Rimmer, General analysis of aplanatic Cassegrain, Gregorian, and Schwarzschild telescopes, Appl. Opt. 11 (12) (1972) 2817–2832.
[3] K. Seidl, J. Knobbe, H. Grüger, Design of an all-reflective unobscured optical-power zoom objective, Appl. Opt. 48 (21) (2009) 4097–4107.
[4] S. Hu, X. Zhao, W. Dong, Y. Xie, Active optical system for any field angle zoom, Opt. Eng. 50 (11) (2011) 1–5.
[5] W. Dong, Y. Xie, E. Li, Design of coaxial catadioptric zoom system using deformable mirrors, Appl. Opt. 3I (6) (2010) 893–896.
[6] Z. Ying, Research on Zoom Lens Design with Liquid Lenses, Changchun Institute of Optics Fine Mechanics and Physics, Chinese Academy of Sciences, 2012.
[7] T. Martinez, D.V. Wick, D.M. Payne, S.R. Restaino, Active optical zoom for laser communication, Proc. SPIE 5793 (2005) 144–147.
[8] D.V. Wick, T. Martinez, Adaptive optical zoom, Opt. Eng. 43 (1) (2004) 8–9.